Advances in Science and Technology Research Journal, 2025, 19(12), 67–80 https://doi.org/10.12913/22998624/210033 ISSN 2299-8624, License CC-BY 4.0

# Published: 2025.11.01

Received: 2025.06.02

Accepted: 2025.10.01

# Tribological characterization of AlTiN, TiN, and TiAlN coatings

Joanna Kowalczyk<sup>1</sup>, Monika Madej<sup>1\*</sup>

- <sup>1</sup> Kielce University of Technology, al. Tysiąclecia Państwa Polskiego 7, 25-314 Kielce, Poland
- \* Corresponding author's e-mail: mmadej@tu.kielce.pl

### **ABSTRACT**

This article presents a comparative analysis of titanium, nitrogen, and aluminum-based coatings, specifically TiN, AlTiN, and TiAlN, in the context of their tribological behavior and application in machining. Tribological friction and wear tests were performed using a ball-on-disc tribometer in rotary motion under dry friction. The specimens consisted of uncoated HS6-5-2C steel discs, HS6-5-2C steel discs coated with AlTiN, TiN, and TiAlN, and 100Cr6 steel balls as counter-samples. The wear of the discs and balls was evaluated via microscopic investigations, which included the analysis of surface geometry, microstructure, and chemical composition within the wear tracks. The differences in morphology and chemical composition revealed by microscopic analysis had a significant influence on the tribological behavior of the coatings. The addition of aluminum to titanium nitride coatings improved the tribological characteristics by reducing linear wear in the case of the AlTiN coating and providing low-friction properties for the TiAlN coating. Furthermore, compared to the other tested coatings, the TiAlN coating exhibited fewer built-up edges and a less developed surface after friction testing. The obtained results indicate that the appropriate selection of coatings is crucial for the efficiency of cutting tools in dry machining.

**Keywords:** AlTiN coating, TiN coating, TiAlN coating, wear, friction, rotational motion.

### **INTRODUCTION**

Machining of hard materials at high speeds without a coolant is a demanding process [1, 2]. Approximately 90% of the total mechanical energy generated during machining is converted into heat, causing a significant temperature increase in the cutting zone [3, 4]. Machining generates rapid temperature increases, reaching approximately 800 °C [1, 5, 6] or exceeding this value [1]. Consequently, coolants are employed. However, the specialized chemical compositions required for coolant effectiveness can have adverse effects on human health and the environment. The most commonly used cutting fluids are water-based or oil-based [7]. Mineral oil-based coolants are toxic to the environment [7, 8], and their degradation process is difficult to control. Thus, dry machining is a compelling alternative [7], enabled by effective anti-wear coatings that enhance machining efficiency and environmental sustainability. The most well-known methods of protecting tools against wear involve applying protective coatings to their surface. Coatings can be applied using physical vapor deposition (PVD) and chemical vapor deposition (CVD) techniques [9], which differ in their application methods based on the coating type, its characteristics, and the substrate material [10]. PVD refers to a vacuum coating process that allows the deposition of solid material as a thin layer on a substrate through evaporation and condensation. The coating temperature in the PVD process is typically below 500 °C. A thin layer of the coated material is deposited on the base material, making it most suitable for finishing applications. In contrast, CVD is a thermally activated process in which gaseous precursors are injected into a reaction chamber for chemical surface reaction and dissociation, resulting in the formation of a potential coating. The substrate temperature is maintained between 800 °C and over 1000 °C. Both deposition methods can create single-layer and multi-layer coatings [10]. PVD coatings exhibit higher hardness, finer grain structures, and smoother surfaces [9], alongside a low coefficient of friction and good wear resistance [11]. They also tend to be free of cracks and possess compressive residual stresses, making them suitable for interrupted cutting operations, such as milling and threading, as well as applications requiring sharp cutting edges, like finishing. Conversely, CVD coatings achieve superior adhesion due to deeper atomic diffusion into the substrate. These thicker, more wear-resistant coatings [9, 12] are typically employed on tools used for turning operations.

Thin, hard coatings ideally possess high hardness and oxidation resistance [1]. Sliding friction induces mechanical stresses and elevated temperatures, which can lead to oxidation. The intricate nature of sliding friction stems from the complex interplay of these factors, which are influenced by the applied load, sliding velocity, and surrounding environmental conditions. The chemical composition has a significant influence on the type and properties of the layer formed during friction, which determines the frictional behavior and thus the wear rate of the coating [1, 2]. This layer acts as a protective barrier, reducing or eliminating direct surface contact in the contact zone. Under ambient conditions (in the atmospheric environment), this layer is typically an oxide formed by the reaction between the coating and oxygen. The oxidation rate depends on the rate of oxygen diffusion into the metal's crystal lattice [13].

One example is the TiAlN coating, which is resistant to oxidation [1], corrosion [10], and wear. This is possible due to the formation of an Al, O<sub>2</sub> layer on the coating surface at high temperatures during dry machining. Using an AlTiN coating with a high Al content can achieve greater oxidation resistance compared to the TiAlN coating. Another example is the titanium nitride (TiN) coating [1]. The TiN coating has been widely used as a coating material for cutting tools since the mid-1960s [13]. It is characterized by high hardness, good adhesion to the substrate, chemical stability, a low coefficient of friction, and high wear resistance [1]. However, its poor oxidation resistance at high temperatures is a major limitation in many applications [13]. Other properties allow them to be widely used on cutting tools, as well as decorative coatings. TiN coatings can be applied to high-speed steel (HSS) tools and cemented carbides, reducing tool wear and extending their service life [14]. Compared to TiAlN coatings, TiN coatings exhibit greater chemical stability, higher hardness, and better oxidation resistance at high

temperatures, resulting in improved machining performance. In contrast, tools with TiAlN coatings provide better wear resistance and can be used at higher cutting temperatures [1]. The wear behavior of TiN, TiAlN, and AlTiN coatings was compared by Aihua et al. [15]. They demonstrated that TiN and TiAlN coatings exhibited lower coefficients of friction and wear rates compared to the AlTiN coating with a high Al content. The TiAlN coating had excellent tribological properties compared to other coatings, with a wear rate lower than that of both TiN and AlTiN coatings. Chinchaniar and Choudhury [16] demonstrated that coated tools can significantly reduce tool wear. They observed a significant reduction in wear of TiAlN-coated tools compared to uncoated tools during the machining of hardened steel, showing satisfactory performance with an increase in cutting speed from 62 to 200 m/min. Niemczewska-Wójcik et al. [17] conducted tribological tests of TiN, TiCN, and TiAlN coatings. The tests were carried out under lubricated conditions with coolant at a load of 10 N. A steel ball was used as the counter-sample. They noted that the highest coefficient of friction was for the TiCN coating, and the lowest for the TiN coating. The highest linear wear was observed for the TiAIN coating, which fractured (was destroyed or worn out) halfway through the tribological test.

This article aimed to compare titanium, nitrogen, and aluminum-based coatings such as TiN, AlTiN, and TiAlN in the context of their frictional properties and wear resistance. Comparative studies were carried out for three single-layer coatings under dry friction conditions. A comprehensive surface analysis before and after friction testing was also performed using confocal microscopy and scanning electron microscopy. The choice of these coatings was dictated by their ability to achieve high hardness while minimizing stress, a property crucial for cutting tool materials. Literature analysis showed that elements such as titanium, chromium, molybdenum, and zirconium improve the hardness of nitride coatings TiN, CrN, ZrN, and carbonitride coatings TiCN. Additionally, TiAlN coatings limit heat flow, which is crucial in machining processes, while TiN coatings contribute to lowering the coefficient of friction. Furthermore, the introduction of aluminum in appropriate proportions improves mechanical properties and oxidation resistance, making these coatings attractive for industrial applications. This work provides new insights into coatings in the context of their application during machining.

#### MATERIALS AND METHODS

#### **Research materials**

For the friction and wear tests, HS6-5-2C steel discs with an AlTiN, TiN, or TiAlN coating were used. The counter-samples were 6 mm diameter 100Cr6 steel balls. Table 1 summarizes the key parameters of the coatings. All coatings were applied using the PVD arc evaporation method [18].

### **Tribological tests**

Tribological tests were conducted on a TRB3 tribotester under the conditions specified in Table 2.

#### **Surface characteristics**

During the friction and wear tests, the coefficients of friction and linear wear were recorded. Since linear wear measurements represent the combined wear of both the disc and the ball, the individual wear of these components was further quantified using a Leica DCM8 confocal microscope. The surface geometry of the AlTiN, TiN, and TiAlN-coated samples was characterized using a confocal microscope at 20x magnification, yielding isometric images and primary profiles over an area of 2.367 mm by 1.22 mm. The studies were complemented by the observation of wear tracks on the samples and counter-samples

using a Phenom XL scanning electron microscope. This microscope is additionally equipped with an EDS microanalyzer, which was used to examine the chemical composition of the samples in the wear track. The microscope was operated at an accelerating voltage of 15 kV, with a magnification of 1000× for the disc and 300× for the ball.

#### RESEARCH RESULTS AND DISCUSSION

# Surface characteristics before tribological testing

The surface geometry of the AlTiN, TiN, and TiAlN-coated samples are presented in Figure 1. Comparing the coatings, the TiAlN coating had the smoothest surface with the lowest peaks and shallowest valleys. Among the coatings, the TiN coating had the most developed surface. The highest peaks were observed on the uncoated steel disc. This indicates that the application of the tested coatings to the surfaces of HS6-5-2C steel results in a reduction of surface roughness. The surface morphology and chemical composition of the test samples (coated and uncoated discs) and the counter-sample (ball) were also analyzed. These measurements were performed using a Phenom XL scanning electron microscope, as shown in Figure 2. The morphology

**Table 1.** Selected parameters of the investigated coatings [18]

| Coating material | Process temperature, °C | Coating color    | Hardness, GPa | Residual stress,<br>GPa | Max. operating temp. work, °C |  |
|------------------|-------------------------|------------------|---------------|-------------------------|-------------------------------|--|
| AlTiN            | < 600                   | Black and purple | 35 +/- 3      | ~ 0.6                   | 1000                          |  |
| TiAIN            | 500                     | Purple-gray      | 33 +/- 3      | ~ 0.6                   | 900                           |  |
| TiN              | < 500                   | Golden-yellow    | 30 +/- 3      | ~ 0.6                   | 600                           |  |

**Table 2.** The parameters of tribological tests

| Type of motion    | rotary   |
|-------------------|--|
| Load              | P = 10 N   |
| Sliding speed     | v = 0.1 m/s  |
| Friction distance | s = 1000 m   |
| Friction pair     | <ul> <li>disc (uncoated HS6-5-2C steel, HS6-5-2C steel with: TiN, TiAlN or AlTiN coating),</li> <li>ball (100Cr6 steel)</li> </ul> |
| Lubricant         | None   |

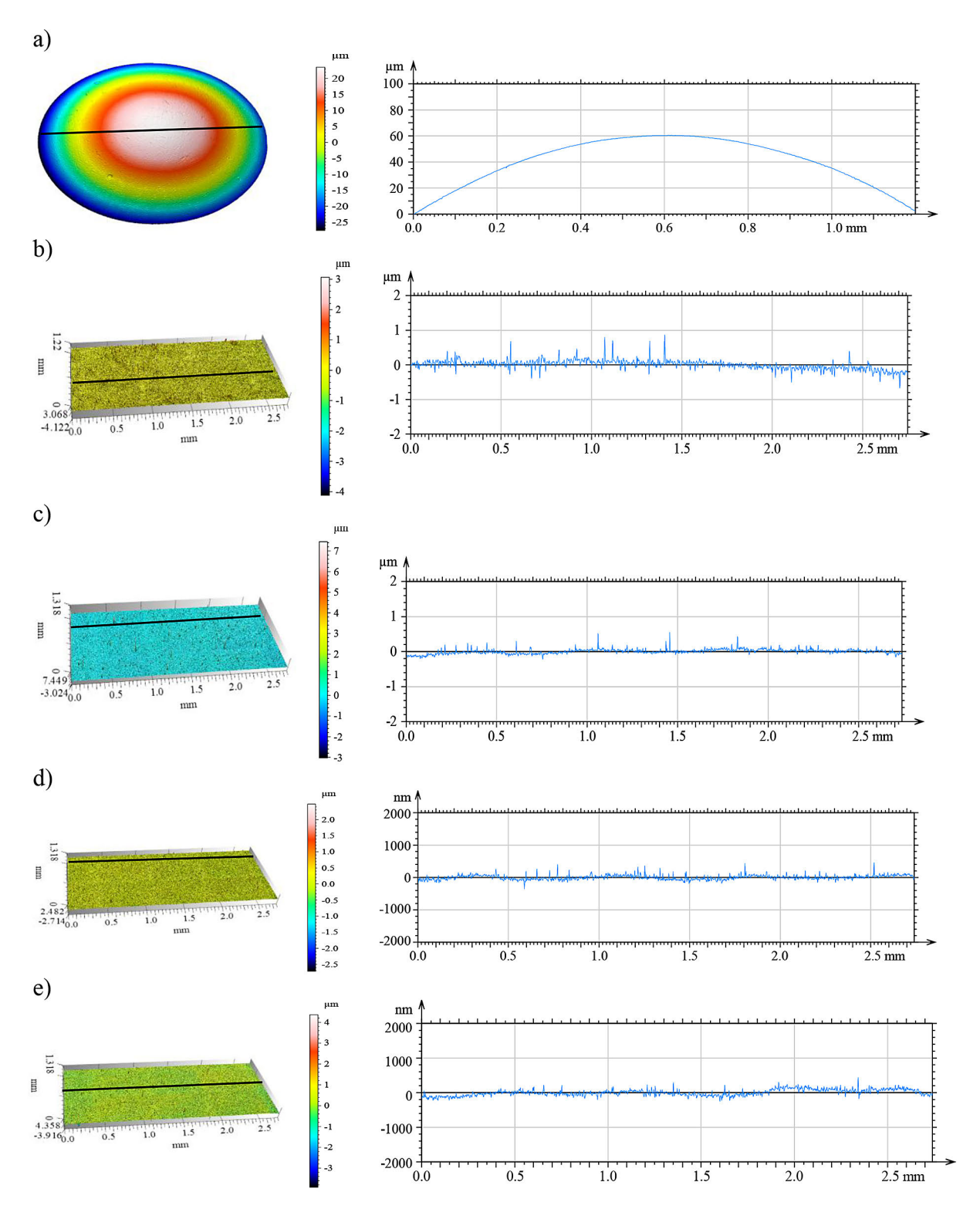


**Figure 1.** Isometric images and primary profiles before tribotests: (a) 100Cr6 steel ball, (b) HS6-5-2C steel, and with coatings: (c) TiN, (d) TiAlN, (e) AlTiN

images of the coated discs revealed non-uniform surfaces, with visible defects like microdroplets, craters, pores, and protrusions [13]. Among the coatings, AlTiN (Figure 2e) displayed the most uniform structure, while TiN (Figure 2c) showed the highest number of defects. To determine the

distribution of elements in a given area, elemental maps were created for the discs, with and without coatings, used in the tribological tests, as shown in Figure 3. The analysis of the test results indicated that the AlTiN coating had the most homogeneous elemental distribution. In contrast, the

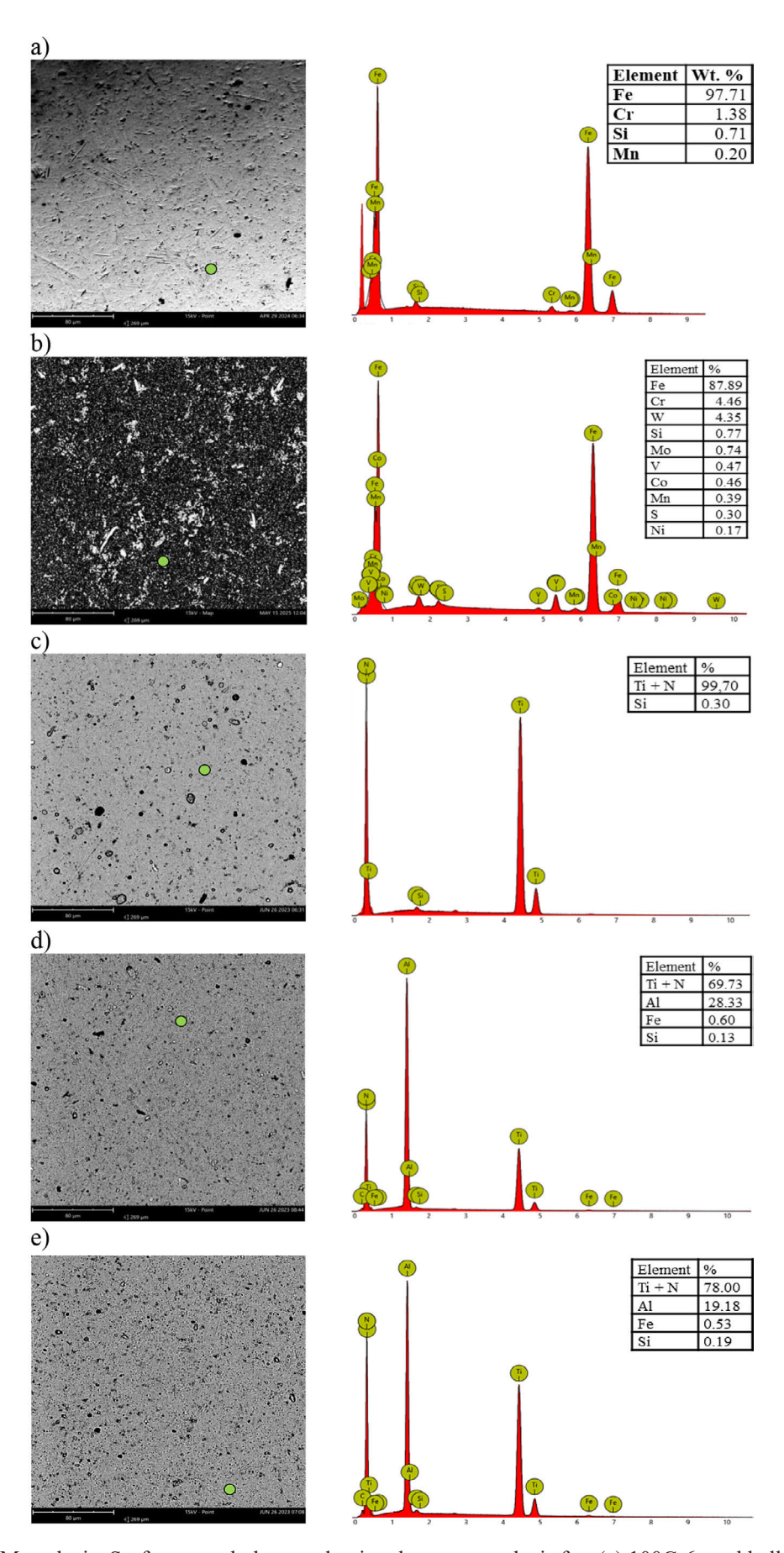


**Figure 2.** SEM analysis: Surface morphology and point elementar analysis for: (a) 100Cr6 steel ball, (b) HS6-5-2C high-speed steel, and coatings: (c) TiN, (d) TiAlN, (e) AlTiN

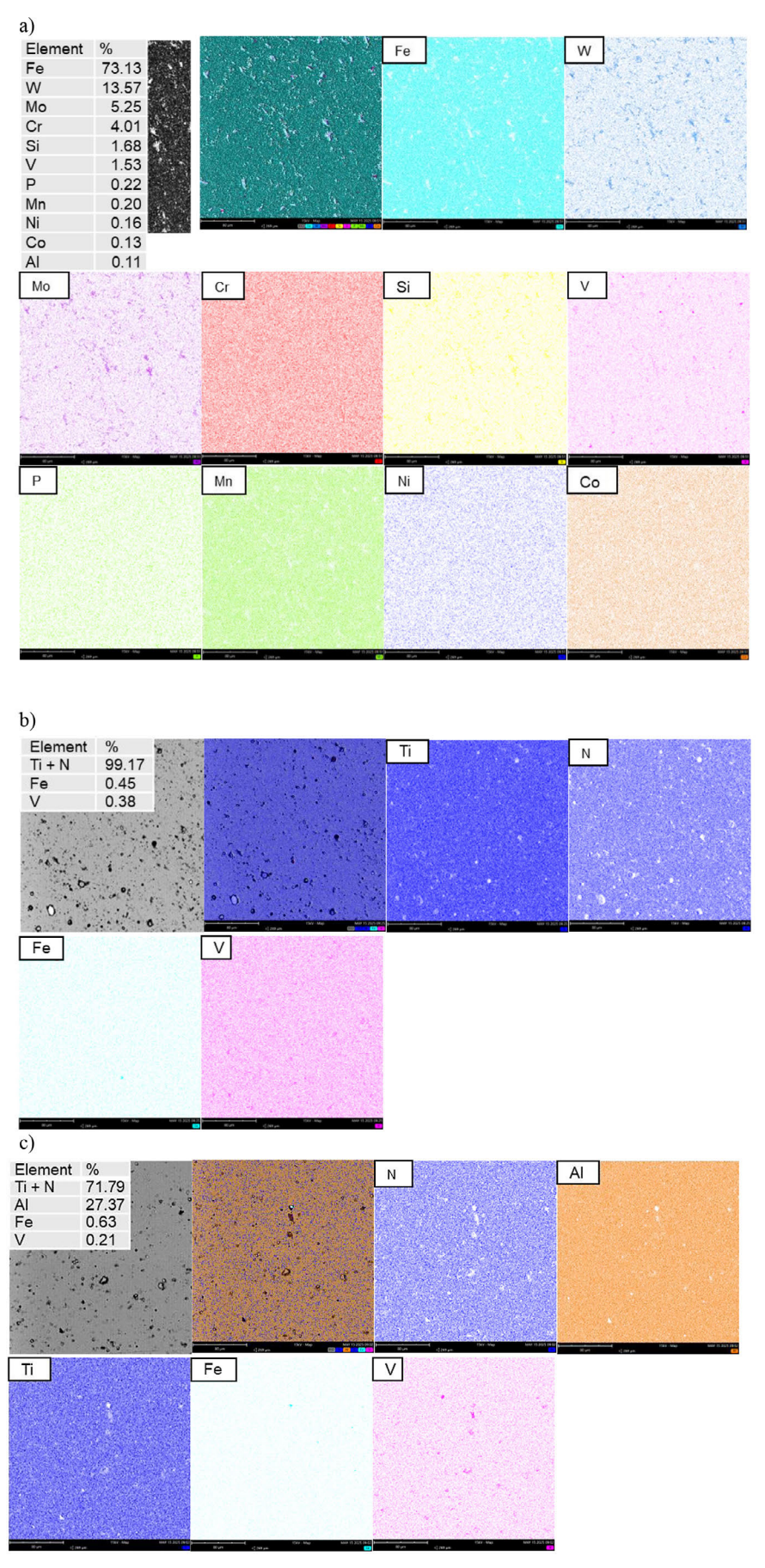


**Figure 3.** Elemental map of samples: (a) HS6-5-2C high-speed steel and coatings: (b) TiN, (c) TiAlN, (e) AlTiN

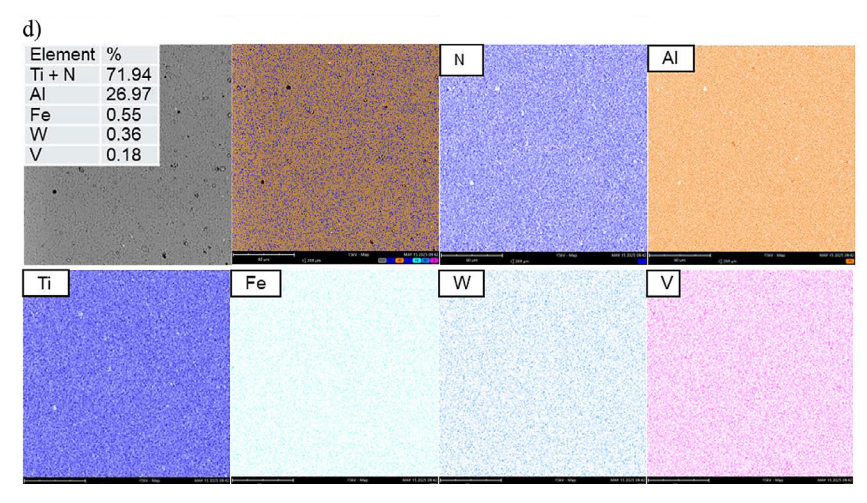


**Figure 3. Cont.** Elemental map of samples: (a) HS6-5-2C high-speed steel and coatings: (b) TiN, (c) TiAlN, (e) AlTiN

TiN and TiAlN coatings showed non-uniformity, with small areas containing substrate elements like iron and vanadium. Similarly, the steel surface displayed an uneven structure with localized regions of tungsten, molybdenum, silicon, and vanadium. To evaluate the tribological performance of these coatings, tests were conducted using a TRB3 tribometer, with the findings summarized in Figure 4. A comparison of the friction and wear characteristics reveals that the lowest coefficient of

friction was recorded for the disc with the TiAlN coating (Figure 4a). Conversely, the highest coefficient was observed for the uncoated steel disc. In contrast, comparing the linear wear plots, the lowest value was observed for the disc with the AlTiN coating, and the highest for TiAlN (Figure 4b). The difference between them was approximately 30%. After the tribological tests, the wear tracks were analyzed using scanning electron microscopy (SEM), energy-dispersive spectroscopy (EDS),

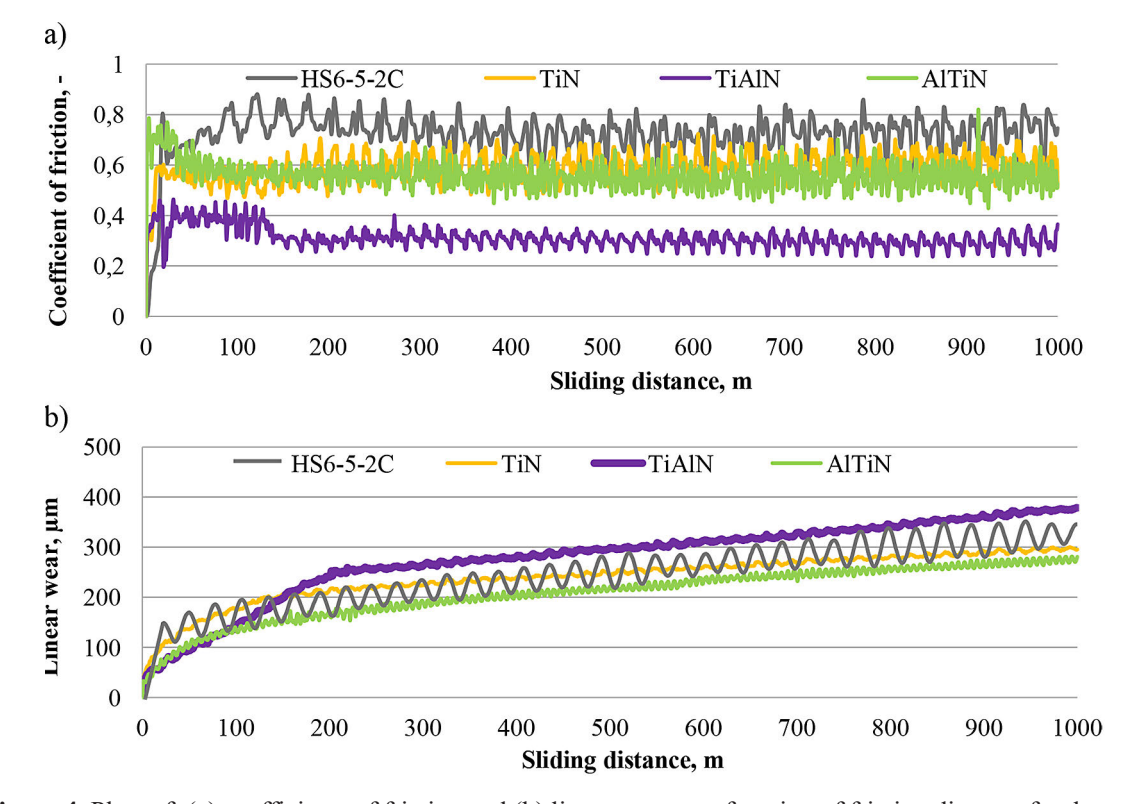


**Figure 4.** Plots of: (a) coefficients of friction and (b) linear wear as a function of friction distance for the tested friction pairs under dry friction conditions

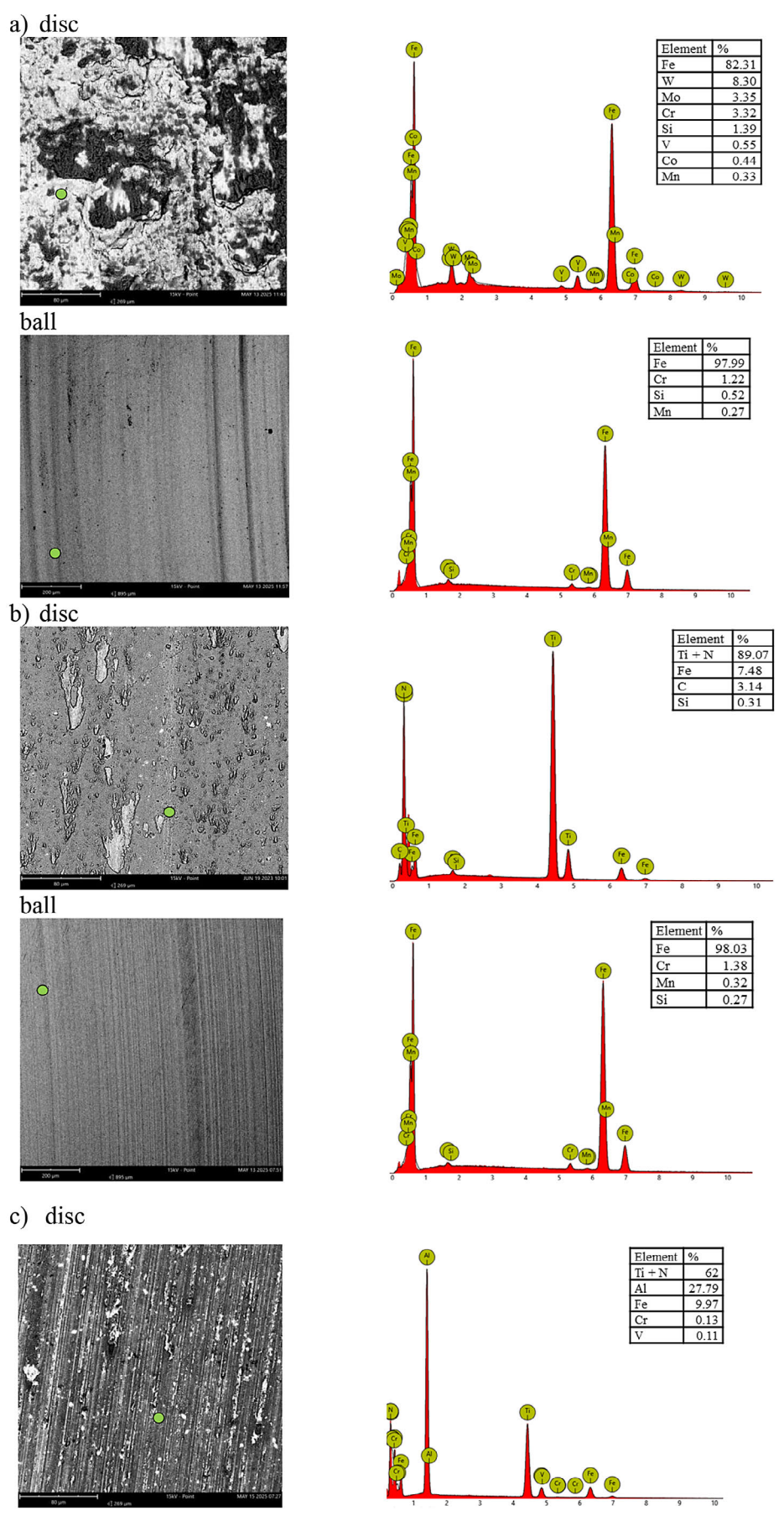


**Figure 5.** SEM: surface morphology with point analysis of samples after tribotests: (a) HS6-5-2C high-speed steel and coatings: (b) TiN, (c) TiAlN, (e) AlTiN

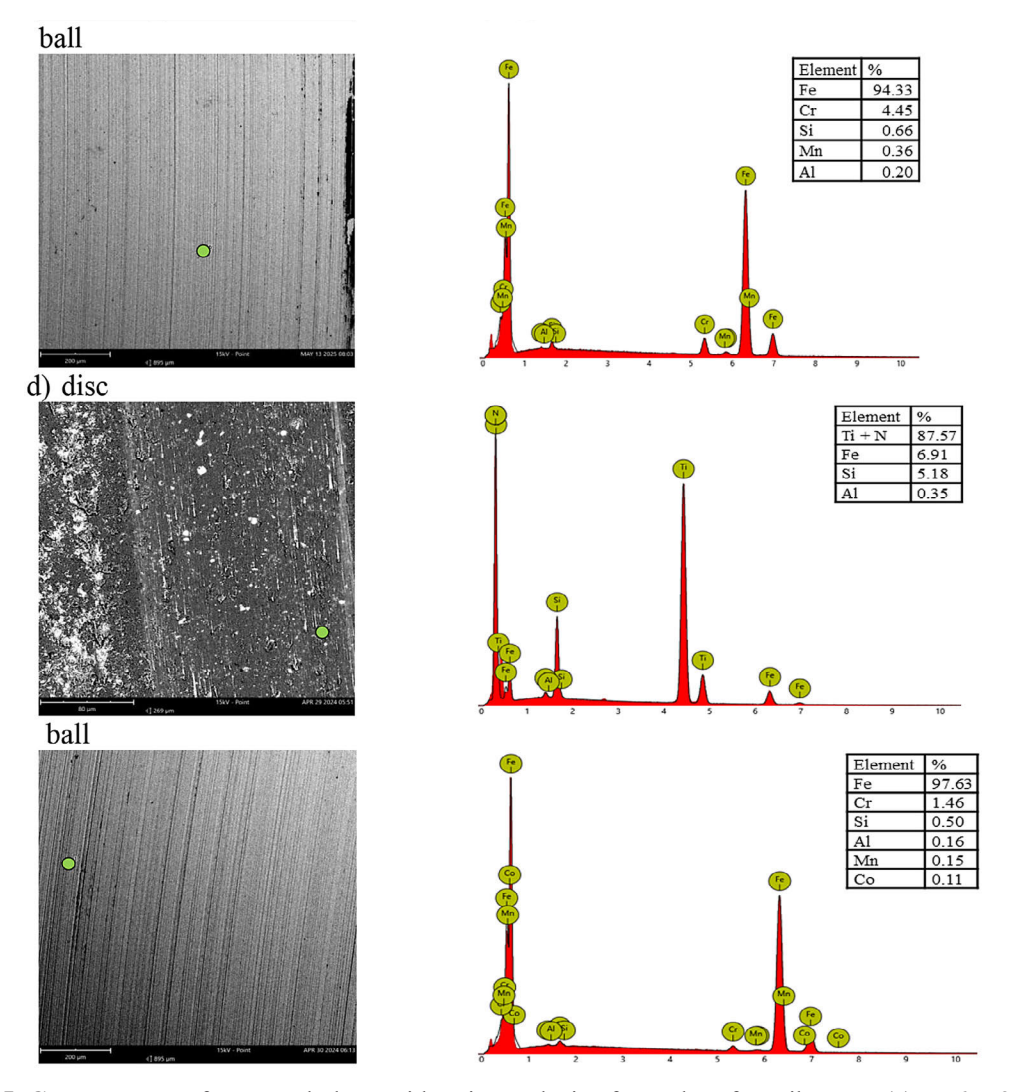


**Figure 5. Cont.** SEM: surface morphology with point analysis of samples after tribotests: (a) HS6-5-2C high-speed steel and coatings: (b) TiN, (c) TiAlN, (e) AlTiN

and confocal microscopy. Images of the surface morphology and the determined chemical composition at the wear track for both discs and balls are summarized in Figure 5.

SEM images revealed built-up edges (appearing as bright areas) on all analyzed coating surfaces. In the wear track of the AlTiN-coated disc, fine wear particles, which contribute to scratches and grooves, suggest an abrasive wear mechanism. Similarly, the TiN-coated disc (Figure 5b) showed numerous built-up edges of varying sizes, and the TiAlN-coated disc also exhibited built-up edges along with fine particles, which influenced the formation of scratches and grooves. To analyze the chemical composition of these built-up edges, elemental maps of both worn and unworn areas were created (Figure 6).

The images obtained indicated the formation of grooves and built-up edges on the coating surfaces, primarily composed of iron, chromium, and vanadium. Conversely, the constituent elements of each coating were distributed across the entire disc surface. On the uncoated steel disc, chromium and tungsten were detected in the deepest section of the wear track. Since the linear wear results from the tribotester are the total wear of the disc and the ball, the wear tracks were additionally examined using a confocal microscope to determine the amount of wear on the discs and balls (Figure 7).

Confocal microscopy revealed that the Al-TiN coating paired with the 100Cr6 steel ball resulted in the narrowest wear track. This combination also exhibited the lowest maximum depth, pit area, and peak area on the disc (Figure 7d). Conversely, the ball interacting with the TiAlN-coated disc displayed the most wear. Its corresponding disc showed the largest pit area

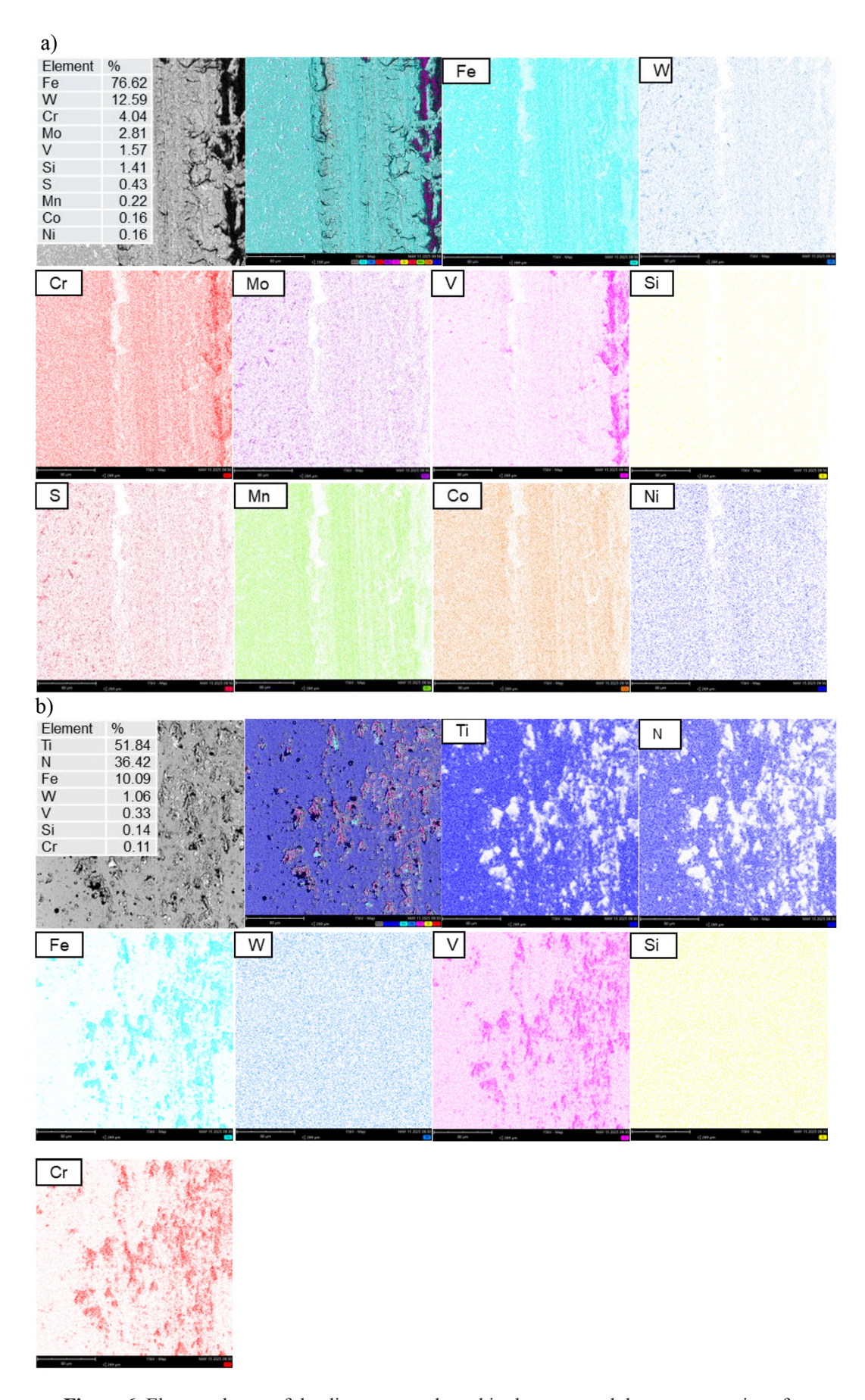


**Figure 6.** Elemental map of the disc area conducted in the worn and the unworn regions for: (a) HS6-5-2C steel and coatings, (b) TiN, (c) TiAlN, (d) AlTiN

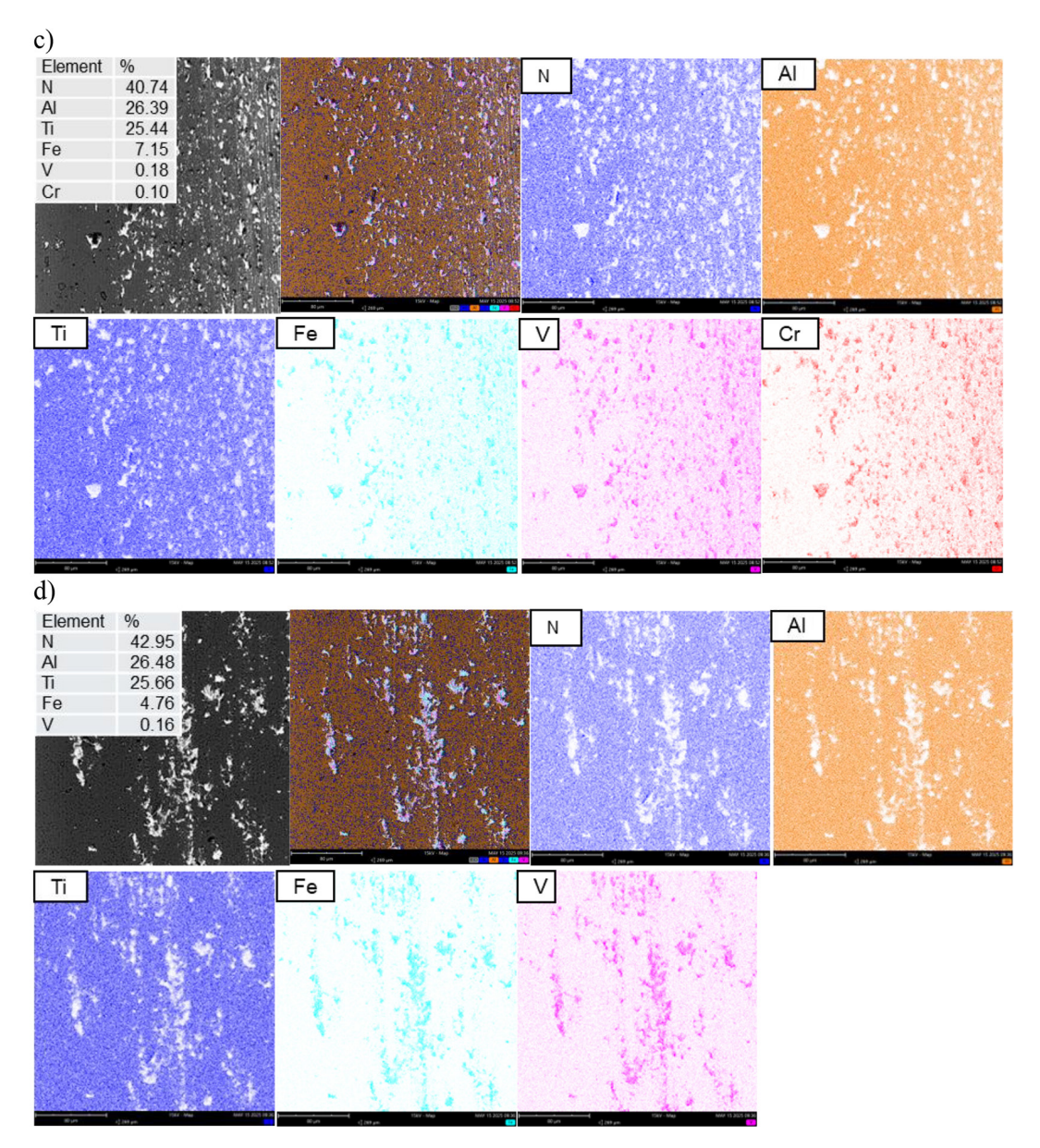


**Figure 6. Cont.** Elemental map of the disc area conducted in the worn and the unworn regions for: (a) HS6-5-2C steel and coatings, (b) TiN, (c) TiAlN, (d) AlTiN

and maximum height (Figure 7c). This suggests the presence of built-up edges on the TiAlN coating that don't fully cover the wear track, as these indentations correspond to the coating's surface. In contrast, the AlTiN coating showed high peak areas and a small pit area, indicating that built-up edges formed across nearly the entire wear track width. This suggests that TiAlN has a lower propensity for built-up edge formation compared to AlTiN. Table 3 summarizes the surface roughness parameters of the samples and counter-samples before and after the tribological tests. Comparing the surface roughness parameters of the discs (Table 3) after the dry friction tribotest revealed that the TiAlN-coated disc

exhibited the lowest Ssk, Sku, Sp, and Sz values. The lowest values of the Sa and Sq parameters were recorded for the disc with the TiN coating. Analyzing the balls revealed the lowest Sq, Sp, and Sa values for the ball paired with the TiAlN-coated disc. In contrast, the other balls showed significant increases (over 80%) in Sp, Sv, and Sz, suggesting the development of surface irregularities (peaks and valleys). Additionally, their Sa values rose by about 96%, indicating a lack of surface smoothing. The roughness of the coated discs remained relatively stable after the tribotests. A smoothing effect was observed, evidenced by the reduction in peak-related parameters (Sp, Ssk, Sku, Sv, and Sz). Conversely,

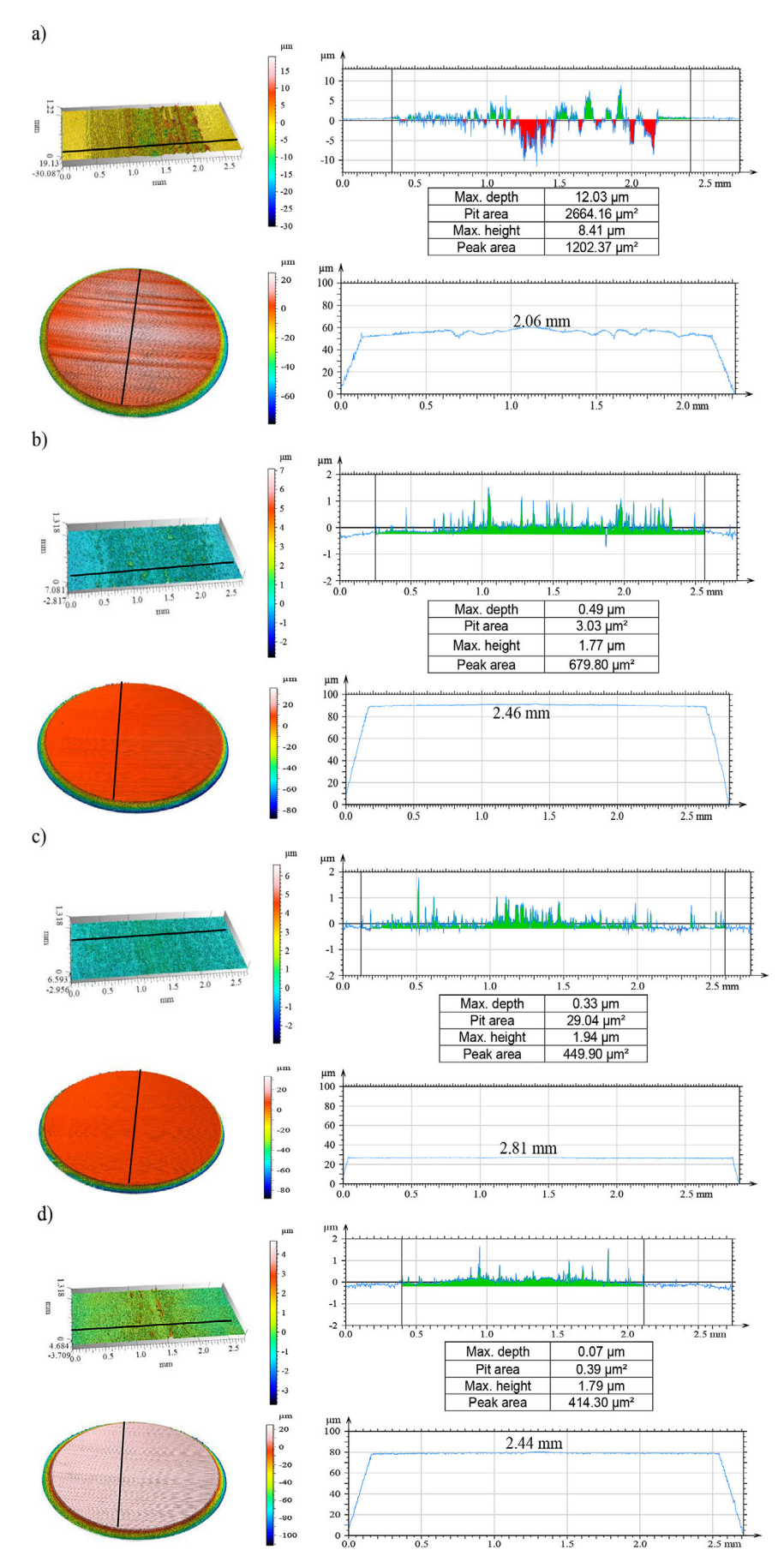


**Figure 7.** Isometric images and primary profiles of discs and balls after tribological tests for: (a) HS6-5-2C hight-speed steel and coatings: (b) TiN, (c) TiAlN, (e) AlTiN

| Table | 3. | Roughness | narameters |
|-------|----|-----------|------------|
| Lanc  | ~. | Nougimess | Darameters |

| The surface roughness parameters |    | New    |          |        |       | ттѕ   |                 |       |            |       |              |       |              |       |
|----------------------------------|----|--------|----------|--------|-------|-------|-----------------|-------|------------|-------|--------------|-------|--------------|-------|
|                                  |    | 100Cr6 | HS6-5-2C | TiN    | TiAIN | AITiN | HS6-5-2C/100Cr6 |       | TiN/100Cr6 |       | TiAIN/100Cr6 |       | AlTiN/100Cr6 |       |
|                                  |    | ball   | disc     | disc   | disc  | disc  | disc            | ball  | disc       | ball  | disc         | ball  | disc         | ball  |
| Sq                               | μm | 0.30   | 0.40     | 0.14   | 0.18  | 0.33  | 4.18            | 6.00  | 0.28       | 8.47  | 0.29         | 0.19  | 0.76         | 8.02  |
| Ssk                              |    | 0.22   | -0,00    | 7.61   | 2.13  | 1.23  | -0.09           | 0.31  | 2.50       | 0.07  | 0.45         | -0.03 | 0.59         | 0.35  |
| Sku                              |    | 6.33   | 2.57     | 140.00 | 13.53 | 21.92 | 2.99            | 2.43  | 10.29      | 1.88  | 2.98         | 3.84  | 4.38         | 2.32  |
| Sp                               | μm | 3.04   | 2.90     | 4.74   | 1.36  | 6.97  | 17.50           | 21.63 | 2.57       | 18.13 | 1.31         | 1.99  | 6.46         | 22.27 |
| Sv                               | μm | 2.77   | 2.05     | 2.68   | 1.59  | 4.35  | 32.40           | 23.71 | 1.39       | 14.76 | 1.43         | 4.68  | 3.46         | 14.38 |
| Sz                               | μm | 5.81   | 4.94     | 7.42   | 2.95  | 11.32 | 49.99           | 45.34 | 3.96       | 32.89 | 2.74         | 6.67  | 9.92         | 36.65 |
| Sa                               | μm | 0.23   | 0.33     | 0.06   | 0.11  | 0.22  | 3.34            | 5.01  | 0.17       | 7.29  | 0.23         | 0.15  | 0.59         | 6.71  |

the uncoated steel disc exhibited a significant increase (up to 90%) in all roughness parameters (Sq, Sz, and Sv) post-testing. This high Sz value signifies considerable height variations within the wear track [19], while the elevated Sq value indicates a rough wear surface with numerous irregularities and peaks [20].

#### **CONCLUSIONS**

The research revealed that the TiAlN coating exhibited the fewest defects, suggesting superior quality. Its minimal surface development, as shown by roughness analysis, is beneficial for friction reduction. TiAlN also presented the lowest friction coefficient, making it well-suited for low-friction applications. However, the counter-ball paired with TiAlN experienced the most wear compared to those tested against TiN and AlTiN. Furthermore, TiAlN demonstrated resistance to built-up edge formation, unlike AlTiN and TiN, where larger built-up edges were observed, which could impact its lifespan. Conversely, AlTiN displayed the lowest linear wear, indicating high abrasion resistance, and showed the narrowest wear track with the smallest built-up edges, suggesting effectiveness in machining. Overall, AlTiN exhibited the highest wear resistance under dry friction, making it appropriate for dry machining cutting tools.

## **REFERENCES**

- Çalışkan H., Karaoglanli A. Oxidation behavior of AlTiN/TiN nanolayer hard coating at high temperatures. Acta Phys. Pol. A. 2014; 125: 456–8. https:// doi.org/10.12693/APhysPolA.125.456
- 2. Sivaiah P., Chakradhar D., Narayanan R.G.

- Chapter 4 Sustainable manufacturing strategies in machining. In: Narayanan RG, Gunasekera JS, editors. Sustain. Manuf. Process., Academic Press; 2023, 113–54. https://doi.org/10.1016/B978-0-323-99990-8.00013-8
- Zhao J., Liu Z., Wang B., Hu J., Wan Y. Tool coating effects on cutting temperature during metal cutting processes: Comprehensive review and future research directions. Mech. Syst. Signal Process. 2021; 150: 107302. https://doi.org/10.1016/j. ymssp.2020.107302
- Pereira Guimarães B.M., da Silva Fernandes C.M., Amaral de Figueiredo D., Correia Pereira da Silva F.S., Macedo Miranda MG. Cutting temperature measurement and prediction in machining processes: comprehensive review and future perspectives. Int. J. Adv. Manuf. Technol. 2022; 120: 2849–78. https://doi.org/10.1007/s00170-022-08957-z
- 5. Matras A. Surface roughness prediction in the hardened steel ball-end milling by using the artificial neural networks and Taguchi method. Adv. Sci. Technol. Res. J. 2024; 18: 184–94. https://doi.org/10.12913/22998624/177328
- Okada M., Hosokawa A., Tanaka R., Ueda T. Cutting performance of PVD-coated carbide and CBN tools in hardmilling. Int. J. Mach. Tools. Manuf. 2011; 51: 127–32. https://doi.org/10.1016/j.ijmachtools.2010.10.007
- 7. Kowalczyk J., Madej M., Ozimina D. Assessing the exploitation properties of pro-ecological cutting fluid containing zinc aspartate. Eksploat. Niezawodn. 2020; 22: 465–71.
- Szczotkarz N., Adamczuk K., Dębowski D., Gupta M.K. Influence of aluminium oxide nanoparticles mass concentrations on the tool wear values during turning of titanium alloy under minimum quantity lubrication conditions. Adv. Sci. Technol. Res. J. 2024; 18: 76–88. https://doi. org/10.12913/22998624/175917
- 9. Kucharska B., Czarniak P., Kulikowski K., Krawczyńska A., Rożniatowski K., Kubacki J., et

- al. Comparison study of PVD coatings: TiN/AlTiN, TiN and TiAlSiN used in wood machining. Materials. 2022; 15. https://doi.org/10.3390/ma15207159
- Yaqoob S., Ghani J.A., Jouini N., Juri A.Z. Performance evaluation of PVD and CVD multilayer-coated tools in machining high-strength steel. Coatings. 2024; 14. https://doi.org/10.3390/coatings14070865
- 11. Dobrzyński M., Miętka K. Surface texture after turning for various workpiece rigidities. Machines. 2021: 1–10.
- 12. Bobzin K. High-performance coatings for cutting tools. CIRP J. Manuf. Sci. Technol. 2017; 18: 1–9. https://doi.org/10.1016/j.cirpj.2016.11.004
- 13. Liew W.Y.H., Jie J.L.L., Yan L.Y., Dayou J., Sipaut C.S., Madlan M.F.B. Frictional and wear behaviour of AlCrN, TiN, TiAlN single-layer coatings, and TiAlN/AlCrN, AlN/TiN nano-multilayer coatings in dry sliding. Procedia. Eng. 2013; 68: 512–7. https://doi.org/10.1016/j.proeng.2013.12.214
- 14. Qiao H., Liu M., Xiang Y., Xu X., Wang Z., Wu W., et al. Low-friction coatings grown on cemented carbides by modulating the sputtering process parameters of TiN targets. Coatings. 2025; 15. https://doi.org/10.3390/coatings15030329

- Aihua L., Jianxin D., Haibing C., Yangyang C., Jun Z. Friction and wear properties of TiN, TiAlN, AlTiN and CrAlN PVD nitride coatings. Int. J. Refract. Met. Hard. Mater. 2012; 31: 82–8. https://doi. org/10.1016/j.ijrmhm.2011.09.010
- Chinchanikar S., Choudhury S.K. Wear behaviors of single-layer and multi-layer coated carbide inserts in high speed machining of hardened AISI 4340 steel.
   J. Mech. Sci. Technol. 2013; 27: 1451–9. https://doi. org/10.1007/s12206-013-0325-2
- 17. Niemczewska-Wójcik M, Madej M. Surface topography and tribological properties of cutting tool coatings. Adv. Sci. Technol. Res. J. 2023; 17: 39–48. https://doi.org/10.12913/22998624/173214
- 18. Oerlikon Balzers 2025. https://www.oerlikon.com/balzers/pl/pl/
- 19. Wieczorkowski M. Theoretical basis of spatial analysis of surface asperities. Inż. Masz. 2013; 18: 7–34.
- Grzesik W. Effect of the machine parts surface topography features on the machine service. Mechanik. 2015; 8–9: 587–93. http://dx.doi.org/10.17814/ mechanik.2015.8-9.490